Patterned Polypeptoid Brushes

Maximilian Schneider, Zian Tang, Marcus Richter, Claudia Marschelke, Paul Förster, Erik Wegener, Ihsan Amin, Heike Zimmermann, Dieter Scharnweber, Hans-Georg Braun, Robert Luxenhofer,* Rainer Jordan*

Patterned polypeptoid brushes on gold and oxide substrates are synthesized by surface-initiated polymerization of N-substituted glycine *N*-carboxyanhydrides. Their biofouling resistance is shown by protein and cell adhesion experiments. The accessibility of the system to common patterning protocols is demonstrated by UV-lithography and a μCP approach. Moreover, the terminal secondary amine group of the polypeptoid brushes is functionalized with different fluorescent dyes to demonstrate their chemical accessibility.

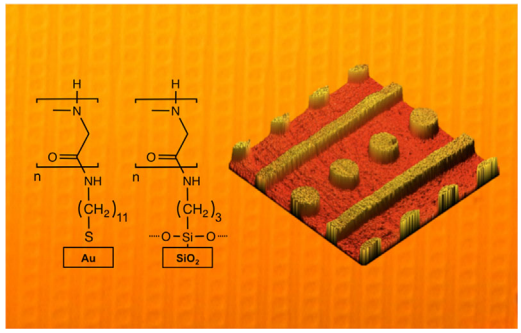

1. Introduction

The capability to control the adsorption of biomolecules is a fundamental issue for a wide range of biotechnological applications. For the control of biofouling, the adsorption of biomolecules and subsequently cells and/or organisms has to be efficiently reduced for coatings of marine vessels,[1] filtration or desalination devices,[2,3] and in many biomedical applications.[4] Whereas selective adsorption has to be promoted for sensor applications[5] or scaffolds used in tissue engineering.[6–8] DNA microarray devices[9] and tissue microarrays[10,11] are further examples of applications where a controlled bio-adhesion is required.

By now, there is a wide range of antifouling coatings available, mostly based on polymers.[12] General design principles for polymers with low protein binding have been established[13,14] and challenged.[15,16] The more common design paradigm is that polymers should be sufficiently hydrophilic and of zero net charge (non-ionic or zwitterionic) and feature H-bond acceptors but no H-bond donors. Polyether-based polymer brush coatings have been very successful in this context and PEGylation remains one of the most commonly applied methods to prevent biofouling of surfaces, particles, aggregates, and even molecular entities with the so-called stealth effect.[17–21] However, a detailed study by Whitesides and Grunze[22] on oligo-(ethlene glycol)-terminated self-assembled monolayers (SAMs) on gold and silver showed that the ability of polyether coatings to resist protein adsorption strongly depends on their molecular conformation and binding of interfacial water to the ethylene glycol units. In recent years though, PEG has come under some scrutiny[23] as PEG as a

R. Jordan, M. Schneider, Z. Tang, M. Richter, C. Marschelke, P. Förster, E. Wegener, I. Amin
Chair of Macromolecular Chemistry, Department of Chemistry and Food Chemistry, School of Science, TU Dresden, Mommsenstr. 4, 01069 Dresden, Germany
E-mail: Rainer.Jordan@tu-dresden.de
Fax: +49 351 463 37122
R. Luxenhofer
Functional Polymer Materials, Chair for Chemical Technology of Materials Synthesis, University Würzburg, Röntgenring 11, 97070 Würzburg, Germany
E-mail: robert.luxenhofer@uni-wuerzburg.de
Fax: +49 931 31 82109
H. Zimmermann, D. Scharnweber, H.-G. Braun
Max-Bergmann Center of Biomaterials Dresden, Budapester Str. 27, 01069 Dresden, Germany

DOI: 10.1002/mabi.201500314

polyether is prone to oxidative degradation[24] leading to "PEG poisoning"[25] and reported failure of PEGylated drugs because of specific recognition of PEG by the immune system.[26–28] Thus alternative polymers are needed, especially if designated for regular or long-term use in humans. In this context, Textor and co-workers have shown that PEG-based coatings exhibit reduced long-term stability as compared to poly(2-oxazoline) (POx)-based coatings.[29,30] Other alternatives are, for example, polyglycerols, which also have shown to exhibit a higher stability as compared to PEG.[31] However, also contradictory studies can be found in this context. For example, Dworak reported that polyglycerols are faster degraded under UV-irradiation in aqueous conditions.[32] Ulbricht et al. reported recently that in solution, POx and polypeptoids are degraded faster than PEG, when subjected in vitro to conditions aimed to mimic phagosomes in activated neutrophils or macrophages.[33]

Polypeptoids (poly(N-substituted glycine) s) are a class of biomimetic polymers that have seen some interest recently.[34,35] Similar to POx, they are constitutional isomers of natural polypeptides.[34,36] In contrast to polypeptides, the polypeptoids are substituted at the amide nitrogen and cannot form intermolecular hydrogen bonds to stabilize secondary structures. Until recently, polysarcosine (poly(*N*-methylglycine)) was the only studied polypeptoid obtained via polymerization in any considerable detail. In the last years, the molecular tool-kit was expanded considerably. Now, hydrophilic, amphiphilic,[37,38] and hydrophobic[39] as well as thermoresponsive[40–42] and reactive[43,44] polypeptoids are available. Polysarcosine shows excellent nonfouling properties and long-circulating drug-delivery systems based on polysarcosine have been reported.[45–47] Polypeptoids are either obtained by iterative sub-monomer solid-phase synthesis[34,48] or by nucleophilic living condensative ring-opening polymerization (NuLCROP) of N-substituted glycine *N*-carboxyanhydrides (NNCAs)[39] or N-substituted glycine *N*-thiocarboxyanhydrides (NNTAs).[42] The NuLCROP allows the preparation of highly defined polypeptoids in solution[49] and on solid supports.[50] Recently, we demonstrated that surface-initiated living condensative ring-opening polymerization (SI-LCROP) of NNCAs from SAMs of 3-(aminopropyl) trimethoxysilane (APTMS) on planar silicon dioxide substrates results in homogeneous hydrophilic, hydrophobic, and amphiphilic polypeptoid brushes.[51] The utilization of an initiating SAM results in dense polymer brushes with an excellent surface screening. SAMs as 2D initiating systems can be readily exploited to prepare patterned polymer brushes by surface-initiated polymerization from SAMs patterned by various techniques.[52] Since polypeptoid brushes are most suitable for the application in biotechnology, the possibility of microscale patterning on different types of substrates is very intriguing for further development.

Here, we demonstrate the resistance of polypeptoids against biofouling and show the synthesis of patterned polypeptoid brushes by different methods on two different types of substrates using patterned SAM-initiators. We demonstrate a top-down photolithographic process as well as a bottom-up micro contact printing (μCP) procedure to obtain patterned polypeptoid brushes on silicon dioxide as well as gold substrates. Furthermore, the polypeptoid brush chain termini were selectively functionalized using activated carboxylic acids of dyes as model compounds. The patterning and reactions are summarized in Scheme 1.

2. Experimental Section

2.1. Materials

Chemicals were purchased from Sigma–Aldrich (Steinheim, Germany) or Acros (Geel, Belgium) and used as received unless otherwise stated. Dry acetonitrile (ACN, extra dry Acroseal) and dimethylformamide (DMF) were transferred and stored in a glove box under nitrogen. Benzonitrile (BN) and triethylamine (TEA) were refluxed over P_4O_{10} (BN) or CaH_2 (TEA) and distilled under argon prior to use. All organic solvents were tested on their water content by a C20 compact coulometer (Mettler-Toledo, Giessen, Germany) and showed a typically water content of less than 30 ppm. The monomer Sar-NCA was prepared according to the procedure published before.[39] *N*-hydroxysuccinimide esters of Cy5 and Oregon Green were purchased from Interchim (Montluçon, France) and used as received. DyLight488-conjugated ChromPure human Albumin was purchased from Jackson ImmunoReasearch (Newmarket, UK) and used as received. FBS serum and PBS tablets were purchased from Gibco, Live Technologies (Carlsbad, USA). The serum was used as received and the PBS solution was prepared by solving the tablets in deionized water according to the instructions of the manufacturer. Only deionized and bidistilled water was used for sample treatment and measurements. Silicon wafers with a 300 nm oxide layer were purchased from Microchemicals (Ulm, Germany). Gold substrates (30 nm gold, 9 nm titanium adhesion layer on silicon wafer) were purchased from G. Albert PVD (Silz, Germany).

2.2. Self-Assembled Monolayers (SAMs)

SAMs from 3-(aminopropyl) trimethoxysilane (APTMS) on silicon wafers were prepared as reported previously[51,53] and patterned by UV-lithography using a TEM grid (1000 mesh thin bar) as the photomask and a 1000 W Hg-short-arc lamp equipped with a 90° beam turner (LOT-QuantumDesign GmbH, Darmstadt, Germany). Irradiation was performed at a distance of approx. 15 cm for 30 min at r.t.

Gold substrates were cleaned twice with ethanol, followed by 15 min oxygen plasma treatment (Harrick, NY, USA). Homogeneous SAMs were prepared by immersing a freshly cleaned gold substrate in a 2 mM 11-amino-1-undecanethiol hydrochloride (AUDT) solution in EtOH overnight. The samples were rinsed extensively with

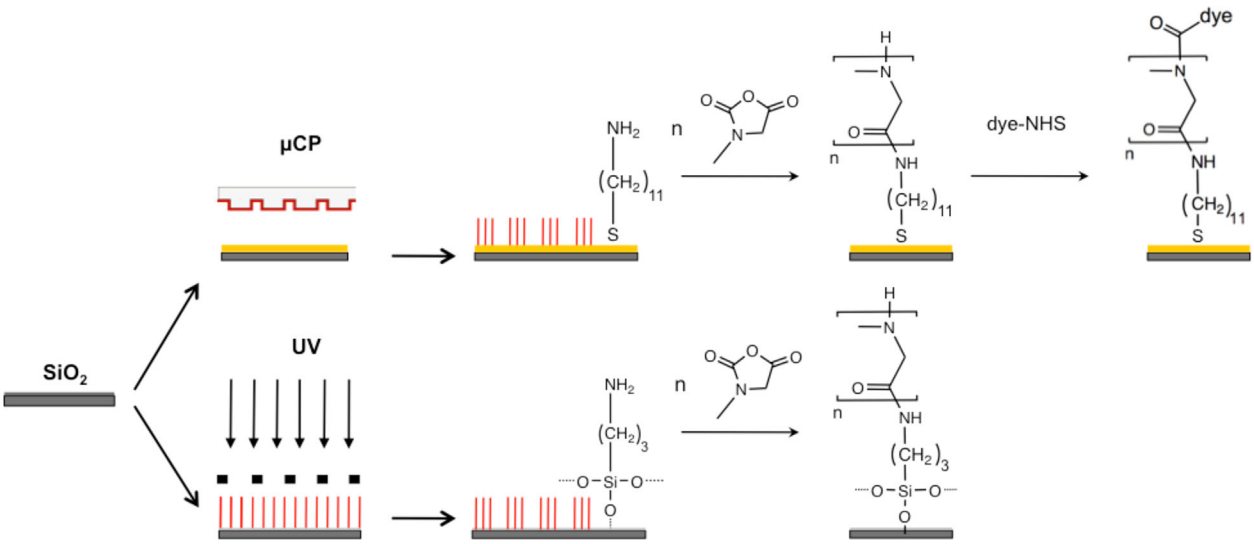

Scheme 1. Patterned SAM initiator surfaces by microcontact printing (top) and UV-lithography (below) and subsequent surface-initiated living condensative ring-opening polymerization (SI-LCROP) of *N*-methyl glycine *N*-carboxyanhydride to patterned polysarcosine brushes. The brush terminal secondary amine was further used for selective functionalization with different dyes as model compounds.

EtOH and dried with argon. Patterned AUDT SAMs were prepared by microcontact printing (μCP) with a PDMS stamp prepared from Sylgard 184 (Dow Corning) on cleaned gold substrates. The stamp was inked with a 2 mM AUDT solution in EtOH, dried a few minutes in air and the excessive solution was removed by a jet of nitrogen. The stamp was carefully placed on the gold substrate applying slight pressure to ensure good contact. The stamp remained in contact for 5 min and was then removed carefully.

2.3. Surface-Initiated Living Condensative Ring-Opening Polymerization (SI-LCROP)

The SI-LCROP was carried out as described previously.[51]

2.4. Polymer Brush End Functionalization

Substrates with patterned polysarcosine brushes were placed in a flame-dried Schlenk-tube with an excess of Cy5-NHS, Cy5-azide, or Oregon Green-NHS (approx. 0.3 mg) dissolved in 2 mL of DMF and 50 μL of TEA as a base. The solution was stirred for over 36 h in the dark at r.t. and then rinsed with DMF, washed with EtOH/water (3:1) and ultrasonicated in EtOH.

2.5. Characterization

The SAM and polymer brushes layer thickness were measured by a Sentech SE 800 spectral ellipsometer (Sentech, Berlin, Germany). Data were fitted using a two-layer model in which the silicon oxide layer and organic layer was represented by a Cauchy model, whereas the gold layer was fitted by a Tauc–Lorentz model for each measurement. As fitting parameters for the organic layer, we used the previously determined values of Messersmith and co-workers.[45,54]

Surface plasmon resonance (SPR) was performed on a custom-made instrument purchased from the Max Planck Institute for Polymer Research (Mainz, Germany). The used glass substrates (LaFSN9) were coated with a 45 nm gold layer and coupled to the prism in Kretschmann-configuration. The data were collected and analyzed by the WASPLAS-software.

Cell adhesion studies were performed with hMSC cells of which 10 000 cells were seeded on homogeneous polypeptoid brushes and bare gold substrates. After 2 h of incubation, the samples were rinsed with PBS and the number of adhered cells was determined by lactate dehydrogenase activity (LDH) assay. To see the influence of FBS serum on the cell adhesion, a second experiment with 10% FBS addition to the culture medium was performed.

Protein adhesion experiments were performed on structured polypeptoid brushes by covering the sample with an Albumin-DyLight488 solution for 30 min. After rinsing with deionized water, the sample was dried with a jet of dry nitrogen and examined under the microscope. The fluorescent images were taken with a Zeiss Axio Observer Z1m microscope, equipped with a green filter set (excitation at 440–470 nm, emission at 525–550 nm).

Atomic force microscopy (AFM) was performed with a custom-made Ntegra Aura/Spectra AFM from NT-MDT (Moscow, Russia) in semi-contact mode using a 100 μm^2 sample scanner and probes with a resonant frequency of 47–150 kHz, and a force constant of 0.35–6.1 $N \cdot m^{-1}$ (NSG 03).

Fluorescence spectroscopy and imaging were performed on the same AFM using a green laser (532 nm) for excitation and a peltier-cooled Andor CCD camera as well as a photomultiplier tube (PMT) for detection. Mapping experiments were performed at 532 nm laser irradiation and detection of reflected light with the PMT scanning an area of 30 μm^2 at a resolution of 256 × 256 pixels. On the same area, scanning fluorescence spectroscopy was performed at a resolution of 32 × 32 spectra on 30 μm^2. For all fluorescence spectra, three scans with a single acquisition time of 0.3 s were accumulated.

The static water contact angle was measured by a DSA10 (Krüss, Hamburg, Germany). The given contact angle presents the average of minimum five measurements on different spots of the sample.

3. Results and Discussion

To show the applicability of the SI-LCROP of NNCAs for diverse patterning techniques, we employed two convergent approaches to obtain patterned polypeptoid brushes. In one approach, patterned SAM initiators were prepared by photolithography of homogeneous SAMs of 3-(aminopropyl) trimethoxysilane (APTMS) using a common TEM grid as the photomask. In another approach, microcontact printing (μCP)[55] of 11-amino-1-undecanethiol hydrochloride (AUDT) on gold was used to directly obtain patterned SAM initiators for the consecutive SI-LCROP of Sar-NCA to patterned polypeptoid brushes. The results of both approaches are summarized in Figure 1.

Both approaches result in well-defined and sharp patterns that match the pattern dimensions of the mask or stamp, respectively.

The polypeptoid brush layer thickness evolution as a function of SI-LCROP time was discussed in previous work.[51] On solid and flat substrates as used in the present work, we cannot reliably determine the degree of polymerization of the surface-bound polymers. However, in a previous account, we investigated the Si-LCROP from solid-phase synthesis resins. Narrow dispersities could be obtained after adjustment of reaction parameters and living polymerization was confirmed also on solid phase.[50] In order to elucidate possible differences for AUDT SAMs on gold as initiators, we performed an analogue study with homogeneous as well as patterned AUDT SAMs. The results are shown in Figure 2.

Similar as reported previously for the SI-LCROP of NNCAs on silane SAM initiators on silicondioxide,[51] the AUDT initiator system resulted in an initially linear height increase of the polymer layer with the polymerization time that levels around 96 h. However, while the SI-LCROP from silane APTMS gave a maximum polysarcosine brush thickness of around 40 nm after 6 d, on AUDT SAMs maximum layer thickness levels around 28 nm after 9 d polymerization time. As apparent from the plot in Figure 2a, the polypeptoid brush height evolution is very similar for printed or adsorbed AUDT SAMs. Despite the slightly thinner PSar brush formation on AUDT SAMs, the polymer brush effectively screens the substrate as evidenced by

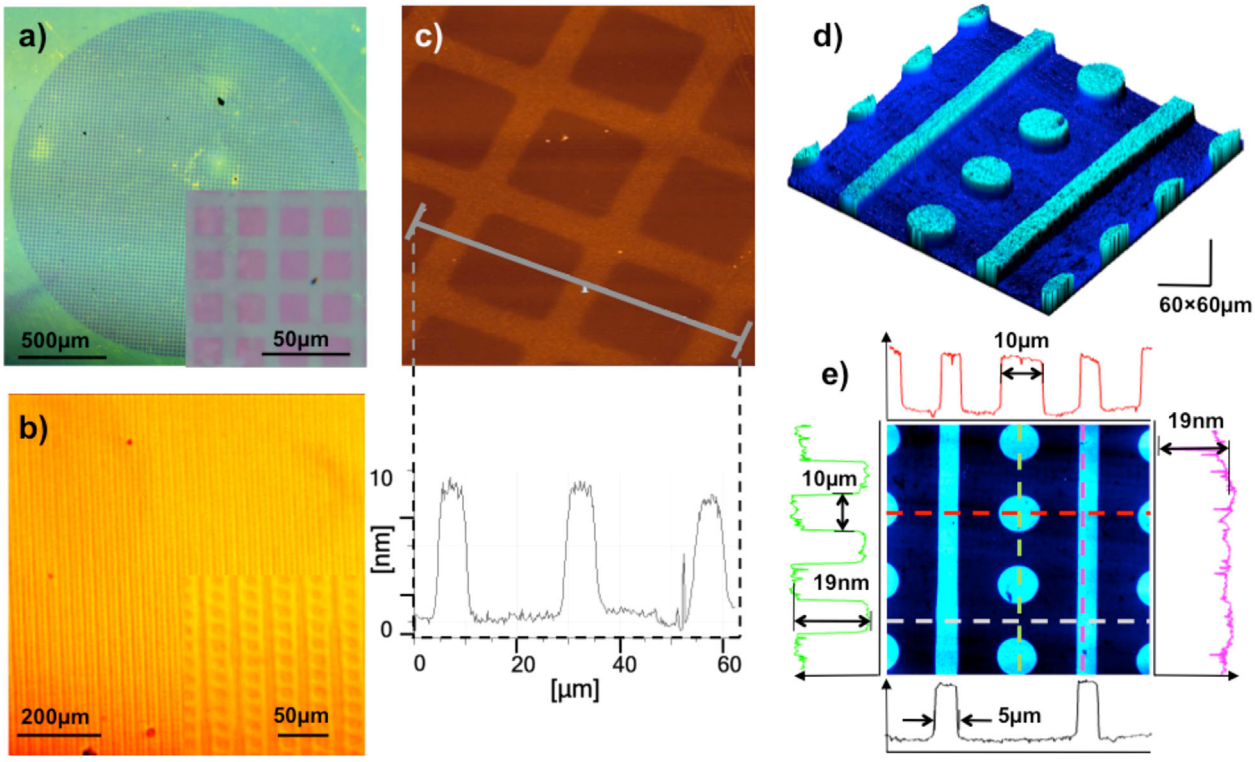

Figure 1. Microscopic images of patterned polysarcosine brushes prepared by (a) UV photolithography of silane SAMs on silicone wafers and (b) μCP of thiols SAMs on gold and consecutive SI-LCROP of Sar-NCA. (c) AFM height scan with height profile of patterned polysarcosine brushes on silicon. (d) AFM height data of a patterned polypeptoid brush on gold (3D) and (e) height analysis of the same scan at lines indicated.

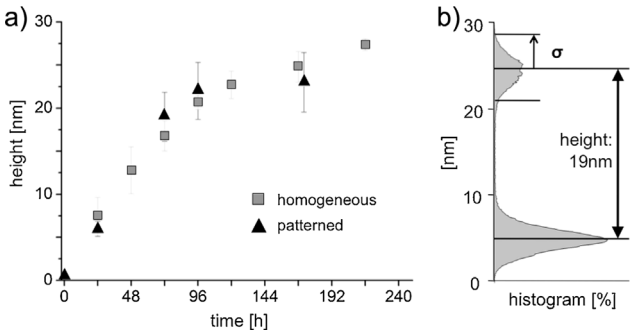

Figure 2. (a) Polysarcosine brush layer thickness as a function of the SI-LCROP time with homogeneous and patterned AUDT SAMs on gold. Please note that each data point was obtained from an individual experiment. Layer thickness was measured by AFM for patterned and by ellipsometry for homogeneous samples. (b) Histogram of the AFM height data of a patterned sample after 72 h of polymerization (from sample as shown in Figure 1e).

wetting experiments. The static water contact angle on AUDT was $\theta(\text{AUDT}) = 65 \pm 2^\circ$ and changed to $\theta(\text{PSar}) < 11 \pm 2^\circ$ after the brush formation even for the thinnest brushes (5–7 nm). The wetting behavior of homogeneous PSar brushes prepared from APTMS SAM initiators on silicon dioxide[51] and AUDT SAMs on gold were found to be identical and in both cases a very hydrophilic polymer brush was formed. The very low contact angle is in good agreement with results found by Messersmith and co-workers[45] for dense PSar brushes (0.6–0.8 chains $\cdot$ nm^{-2}) prepared by the grafting onto approach with a degree of polymerization of $n = 20$. This further indicates the formation of dense PSar brushes by SI-LCROP.

The antifouling property of PSar brushes on gold prepared by SI-LCROP was investigated by protein adsorption from pure FBS monitored by surface plasmon resonance (SPR) as well as cell adhesion studies with human mesenchymal stem cells (hMSC) quantified by the LDH assay (Figure 3).

As apparent from the SPR studies, the PSar coating shows the expected antifouling property as no irreversible protein adsorption from pure FBS was found on homogeneous brushes, even in repetitive cycles (Figure 3a, b). The cell adhesion studies confirmed the nonfouling property of PSar (Figure 3c). Neither from standard cell medium nor from cell medium with 10% FBS hMSC adhered permanently on the PSar surface, while on native gold the cell count was found to be high. With serum addition, almost all seeded cells adhered to the bare gold surface, while still no evidence was found for cell adhesion on the polypeptoid brushes.

An adsorption experiment of Albumin-DyLight488 on patterned polypeptoid brushes confirmed the selective adsorption of proteins on the bare gold substrate between the brush structures (Figure 3d).

Functional polypeptoid brushes are accessible by polymerization of functional NNCA monomers or by polymer analogue conversion of the amine polymer chain end. The latter is especially versatile to tailor the physical and chemical properties of the polymer brush surface because of the surface enrichment of chain termini in polymer brushes. From the most common possible reactions, we chose the reaction with *N*-hydroxysuccinimide (NHS) esters to test the presence and accessibility of the secondary amine group of PSar brushes. For detection purposes, we employed NHS esters of two different fluorescence dyes (Cy5-NHS and Oregon Green-NHS; OG-NHS). As control experiment, we chose a Cy5 dye with an azide function as indifferent coupling agent to rule out physisorption. Patterned PSar brushes on gold were reacted with an excess of Cy5-NHS, Cy5-azide, or OG-NHS in DMF with TEA as a base for over 36 h at room temperature. After extensive cleaning, the samples were investigated by confocal fluorescence scanning microscopy (NTEGRA Spectra) using

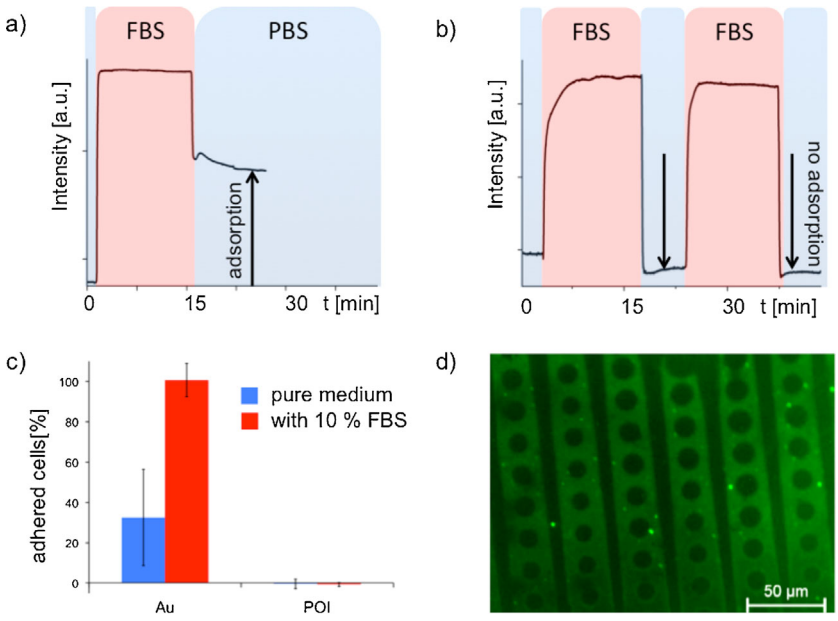

Figure 3. In situ SPR monitoring of protein adsorption from pure FBS on (a) native gold and (b) homogeneous PSar brush ($d = 19.7$ nm) on gold. (c) hMSC cell adhesion on native gold (Au) PSar brush (POI) surfaces from pure culture medium (blue) and with an addition of 10% FBS (red), quantified by the LDH assay. (d) Fluorescence microscopy image of selected absorption of labeled albumin (Albumin-DyLight488) on a patterned PSar brush surface. A surface as depicted in Figure 1b shows strong protein adsorption on areas of native gold but no adsorption on PSar-covered areas (dots and stripes).

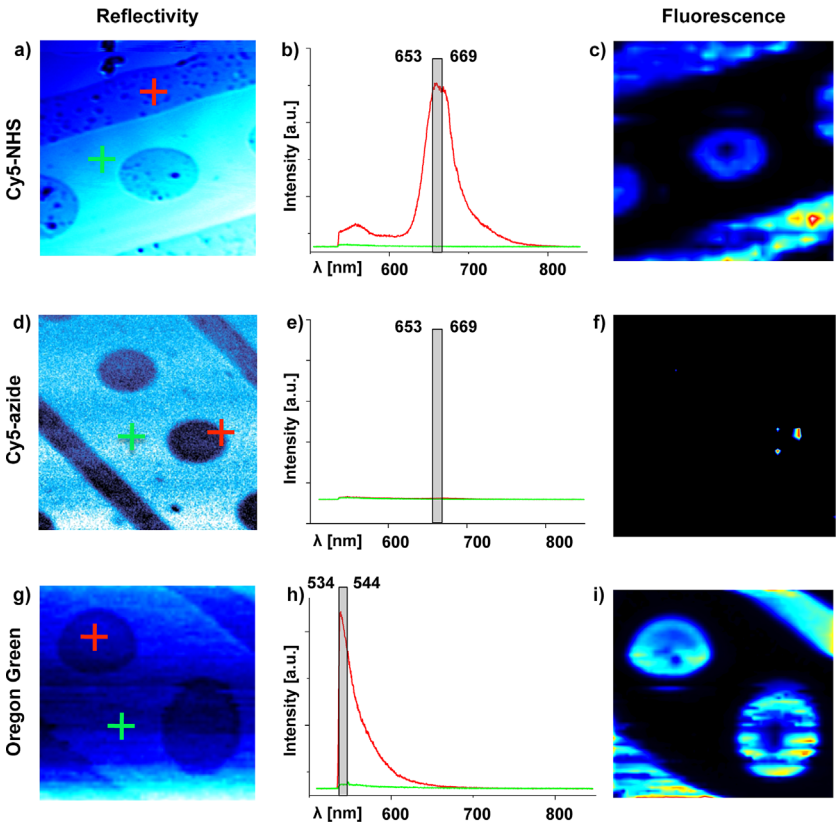

Figure 4. (a) Reflectivity mapping of patterned PSar-Cy5 brushes on gold at a resolution of 256 × 256 pixels on 30 × 30 μm². (b) Fluorescence spectra of PSar-Cy5 recorded at positions as indicated in (a). Only at areas covered by PSar brushes, the typical Cy5 fluorescent emission (600–750 nm) was detected (red mark in (a), red spectrum in (b)). (c) Mapping of the fluorescence intensity in the range of 653–669 nm of patterned PSar-Cy5 at a resolution of 32 × 32 pixels on 30 × 30 μm². (d) Reflectivity mapping of the control sample. Patterned PSar brushes on gold at a resolution of 128 × 128 pixels on 35 × 35 μm². (e) Fluorescence spectra of control sample recorded at positions as indicated in (d). (f) Mapping of the fluorescence intensity in the range of 653–669 nm of the control sample at a resolution of 32 × 32 pixels on 35 × 35 μm². No fluorescent emission of potentially physisorbed dye could be detected. (g) Reflectivity of patterned PSar-OG, (h) fluorescence spectra of PSar-OG recorded at positions as indicated in (g). (i) Mapping of the fluorescence intensity in the range of 534–544 nm of patterned PSar-OG at a resolution of 32 × 32 pixels on 30 × 30 μm². Please note that fluorescent emission of OG lies mainly within the cut-off range of the spectrometer because of the green laser used. However, the fluorescent emission flank is still clearly detectable as apparent in (h).

a 532 nm laser for excitation. With the aid of a first higher resolution reflectivity scan (Figure 4a, d, g; photomultiplier detector), two locations were selected for recording a fluorescence spectrum at a bare and PSar-covered area (Figure 4b, e, h). For both dye-coupling reactions, the typical fluorescence emission could only be detected at the PSar-covered regions. Additionally, the fluorescent intensity of the samples in the spectral range, typical for the respective dyes was mapped over the same sample area (Figure 4c, f, i). Also here, only fluorescent emission on PSar-covered areas were detected which indicates a selective and efficient end functionalization of PSar brushes by the dyes. The control experiment showed that no physisorption occurred during the procedure, since no fluorescent emission could be detected when the sample was reacted with an indifferent dye.

4. Conclusion

We showed the preparation of patterned polypeptoid brushes by surface-initiated living ring-opening polymerization (SI-LCROP) of Sar-NCA on gold and silicon dioxide substrates by patterned self-assembled monolayers prepared by photolithography as well as microcontact printing. Additional studies of the SI-LCROP from homogeneous thiol SAMs on gold showed a similar polymerization behavior of the NNCA as found previously for silane SAMs on silicon dioxide.[51] With protein and cell adhesion experiments, the biofouling resistance of polypeptoid brushes is shown. Finally, the secondary amine group at the polypeptoid brush chain end was found to be readily accessible for chemical functionalization.

Acknowledgement: This work was supported by the Fond der Chemischen Industrie and the Center for Regenerative Therapies Dresden (CRTD). R. J. acknowledge additional support by the Excellence Initiative by the German Federal and State Governments (Institutional Strategy, measure "support the best") through the Dresden Initiative for Bioactive Interfaces & Materials (DIB).

Received: August 18, 2015;
Revised: September 9, 2015; Published online:
DOI: 10.1002/mabi.201500314

Keywords: microstructuring; non-fouling; polymer brush; polysarcosine; surface initiated polymerizition

[1] S. Dobretsov, H. U. Dahms, P. Y. Qian, *Biofouling* **2006**, *22*, 43.
[2] M. Zhou, H. Liu, A. Venkiteshwaran, J. Kilduff, D. G. Anderson, R. Langer, G. Belfort, *J. Mater. Chem.* **2011**, *21*, 693.
[3] R. G. M. van der Sman, H. M. Vollebregt, A. Mepschen, T. R. Noordman, *J. Membr. Sci.* **2012**, *396*, 22.
[4] L. Faxälv, T. Ekblad, B. Liedberg, T. L. Lindahl, *Acta Biomater.* **2010**, *6*, 2599.
[5] J. Davila, D. Toulemon, T. Garnier, A. Garnier, B. Senger, J. C. Voegel, P. Mesini, P. Schaaf, F. Boulmedais, L. Jierry, *Langmuir* **2013**, *29*, 7488.

[6] M. Platen, E. Mathieu, S. Lück, R. Schubel, R. Jordan, S. Pautot, *Biomacromolecules* **2015**, *16*, 1516.
[7] I. M. Wojak-Cwik, V. Hintze, M. Schnabelrauch, S. Moeller, P. Dobrzynski, E. Pamula, D. Scharnweber, *J. Biomed. Mater. Res. A* **2013**, *101*, 3109.
[8] J. Groll, J. Fiedler, E. Engelhard, T. Ameringer, S. Tugulu, H. A. Klok, R. E. Brenner, M. Moeller, *J. Biomed. Mater. Res. A* **2005**, *74*, 607.
[9] M. J. Heller, *Annu. Rev. Biomed. Eng.* **2002**, *4*, 129.
[10] S. R. Ghaemi, F. Harding, B. Delalat, R. Vasani, N. H. Voelcker, *Biomacromolecules* **2013**, *14*, 2675.
[11] J. Kononen, L. Bubendorf, A. Kallionimeni, M. Bärlund, P. Schraml, S. Leighton, J. Torhorst, M. J. Mihatsch, G. Sauter, O.-P. Kallionimeni, *Nat. Med.* **1998**, *4*, 844.
[12] I. Banerjee, R. C. Pangule, R. S. Kane, *Adv. Mater.* **2011**, *23*, 690.
[13] E. Ostuni, R. G. Chapman, R. E. Holmlin, S. Takayama, G. M. Whitesides, *Langmuir* **2001**, *17*, 5605.
[14] H. Vaisocherová, V. Ševců, P. Adam, B. Špačková, K. Hegnerová, A. de los Santos Pereira, C. Rodriguez-Emmenegger, T. Riedel, M. Houska, E. Brynda, J. Homola, *Biosens. Bioelectron.* **2014**, *51*, 150.
[15] C. Rodriguez-Emmenegger, E. Brynda, T. Riedel, M. Houska, V. Šubr, A. B. Alles, E. Hasan, J. E. Gautrot, W. T. Huck, *Macromol. Rapid Commun.* **2011**, *32*, 952.
[16] K. H. A. Lau, T. S. Sileika, S. H. Park, A. M. Sousa, P. Burch, I. Szleifer, P. B. Messersmith, *Adv. Mater. Interfaces* **2015**, *2*, 1400225.
[17] M. C. Woodle, K. K. Matthay, M. S. Newman, J. E. Hidayat, L. R. Collins, C. Redemann, F. J. Martin, D. Papahadjopoulos, *BBA-Biomembranes* **1992**, *1105*, 193.
[18] A. Abuchowski, J. R. McCoy, N. C. Palczuk, T. van Es, F. F. Davis, *J. Biol. Chem.* **1977**, *252*, 3582.
[19] J. M. Harris, N. E. Martin, M. Modi, *Clin. Pharmacokinet.* **2001**, *40*, 539.
[20] X. G. Zhang, D. Y. Teng, Z. M. Wu, X. Wang, Z. Wang, D. M. Yu, C. X. Li, *J. Mater. Sci. Mater. Med.* **2008**, *19*, 3525.
[21] A. Hucknall, S. Rangarajan, A. Chilkoti, *Adv. Mater.* **2009**, *21*, 2441.
[22] P. Harder, M. Grunze, R. Dahint, G. M. Whitesides, P. E. Laibinis, *J. Phys. Chem. B* **1998**, *102*, 426.
[23] M. Barz, R. Luxenhofer, R. Zentel, M. J. Vicent, *Polym. Chem.* **2011**, *2*, 1900.
[24] C. W. McGary, *J. Polym. Sci.* **1960**, *46*, 51.
[25] D. A. Herold, K. Keil, D. E. Bruns, *Biochem. Pharmacol.* **1989**, *38*, 73.
[26] T. Ishida, M. Ichihara, X. Wang, K. Yamamoto, J. Kimura, E. Majima, H. Kiwada, *J. Control. Release* **2006**, *112*, 15.
[27] J. K. Armstrong, G. Hempel, S. Koling, L. S. Chan, T. Fisher, H. J. Meiselman, G. Garratty, *Cancer* **2007**, *110*, 103.
[28] A. A. van der Eijk, J. M. Vrolijk, B. L. Haagmans, *New Engl. J. Med.* **2006**, *354*, 1323.
[29] B. Pidhatika, M. Rodenstein, Y. Chen, E. Rakhmatullina, A. Mühlebach, C. Acikgöz, M. Textor, R. Konradi, *Biointerphases* **2012**, *7*, 1.
[30] R. Konradi, C. Acikgoz, M. Textor, *Macromol. Rapid Commun.* **2012**, *33*, 1663.
[31] M. Lange, S. Braune, K. Luetzow, K. Richau, N. Scharnagl, M. Weinhart, A. T. Neffe, F. Jung, R. Haag, A. Lendlein, *Macromol. Rapid Commun.* **2012**, *33*, 1487.
[32] A. Utrata-Wesolek, R. Trzcińska, K. Galbas, B. Trzebicka, A. Dworak, *Polym. Degrad. Stabil.* **2011**, *96*, 907.
[33] J. Ulbricht, R. Jordan, R. Luxenhofer, *Biomaterials* **2014**, *35*, 4848.
[34] R. Luxenhofer, C. Fetsch, A. Grossmann, *J. Polym. Sci. A* **2013**, *51*, 2731.
[35] C. Secker, S. M. Brosnan, R. Luxenhofer, H. Schlaad, *Macromol. Biosci.* **2015**, *15*, 881.
[36] R. Luxenhofer, S. Huber, J. Hytry, J. Tong, A. V. Kabanov, R. Jordan, *J. Polym. Sci. A* **2013**, *51*, 732.
[37] C. Fetsch, R. Luxenhofer, *Macromol. Rapid Commun.* **2012**, *33*, 1708.
[38] C. Fetsch, S. Flecks, D. Gieseler, C. Marschelke, J. Ulbricht, K.-H. van Pée, R. Luxenhofer, *Macromol. Chem. Phys.* **2014**, *216*, 547.
[39] C. Fetsch, A. Grossmann, L. Holz, J. F. Nawroth, R. Luxenhofer, *Macromolecules* **2011**, *44*, 6746.
[40] S. H. Lahasky, X. Hu, D. Zhang, *ACS Macro Lett.* **2012**, *1*, 580.
[41] J. W. Robinson, C. Secker, S. Weidner, H. Schlaad, *Macromolecules* **2013**, *46*, 580.
[42] X. Tao, J. Du, Y. Wang, J. Ling, *Polym. Chem.* **2015**, *6*, 3164.
[43] C. Secker, J. W. Robinson, H. Schlaad, *Eur. Polym. J.* **2015**, *62*, 394.
[44] S. H. Lahasky, W. K. Serem, L. Guo, J. C. Garno, D. Zhang, *Macromolecules* **2011**, *44*, 9063.
[45] K. H. Lau, C. Ren, T. S. Sileika, S. H. Park, I. Szleifer, P. B. Messersmith, *Langmuir* **2012**, *28*, 16099.
[46] H. Tanisaka, S. Kizaka-Kondoh, A. Makino, S. Tanaka, M. Hiraoka, S. Kimura, *Bioconjug. Chem.* **2008**, *19*, 109.
[47] A. Makino, S. Kizaka-Kondoh, R. Yamahara, I. Hara, T. Kanzaki, E. Ozeki, M. Hiraoka, S. Kimura, *Biomaterials* **2009**, *30*, 5156.
[48] J. Sun, R. N. Zuckermann, *ACS Nano* **2013**, *7*, 4715.
[49] C. Fetsch, R. Luxenhofer, *Macromol. Rapid Commun.* **2012**, *33*, 1708.
[50] N. Gangloff, C. Fetsch, R. Luxenhofer, *Macromol. Rapid Commun.* **2013**, *34*, 997.
[51] M. Schneider, C. Fetsch, I. Amin, R. Jordan, R. Luxenhofer, *Langmuir* **2013**, *29*, 6983.
[52] T. Chen, I. Amin, R. Jordan, *Chem. Soc. Rev.* **2012**, *41*, 3280.
[53] N. Zhang, T. Pompe, I. Amin, R. Luxenhofer, C. Werner, R. Jordan, *Macromol. Biosci.* **2012**, *12*, 926.
[54] K. H. A. Lau, C. Ren, S. H. Park, I. Szleifer, P. B. Messersmith, *Langmuir* **2012**, *28*, 2288.
[55] Y. Xia, G. M. Whitesides, *Angew. Chem. Int. Ed.* **1998**, *37*, 550.